Å upon *complete* $^6A \rightarrow {}^2T$ conversion, whereas for a $^5A \rightarrow {}^1A$ process in the $[Fe^{II}(6\text{-}Mepy)_n(py)_m tren]^{2+}$ series,[36] the average Fe–N distances may change by as much as ~0.25 Å. Thus, for these two spin-equilibrium series, the larger hs → ls geometry change found in the iron(II) complexes seems consistent with the observed slower spin-interconversion rates in both the solid (Mössbauer $k < 10^7 s^{-1}$ [36]) and solution states (laser T-jump $k \simeq 5 \times 10^6 s^{-1}$ [16]) as compared to the Fe-(dtc)$_3$'s (Mössbauer $k > 10^7 s^{-1}$;[9] laser T-jump $k > 10^7 s^{-1}$ [18]) with their correspondingly smaller coordination sphere reorganization. It will be interesting to see if future studies continue to support this view.

References and Notes

(1) Robert A. Welch Predoctoral Fellow.
(2) National Science Foundation Postdoctoral Fellow 1976–1977.
(3) L. Cambi and A. Cagnosso, *Atti Accad. Naz. Lincei, Cl. Sci. Fis., Mat. Nat., Rend.*, [6] **13**, 809 (1931); L. Cambi and L. Szego, *Ber. Dtsch. Chem. Ges. A*, **64**, 2591 (1931).
(4) R. L. Martin and A. H. White, *Transition Met. Chem.*, **4**, 113 (1968).
(5) R. Chant, A. R. Hendrickson, R. L. Martin, and N. M. Rohde, *Inorg. Chem.*, **14**, 1894 (1975).
(6) E. K. Barefield, D. H. Busch, and S. M. Nelson, *Q. Rev., Chem. Soc.*, **22**, 457 (1968).
(7) L. Saconi, *Pure Appl. Chem.*, **27**, 161 (1971).
(8) P. B. Merrithew and P. G. Rasmussen, *Inorg. Chem.*, **11**, 325 (1972).
(9) G. R. Hall and D. N. Hendrickson, *Inorg. Chem.*, **15**, 607 (1976).
(10) J. G. Leipoldt and P. Coppens, *Inorg. Chem.*, **12**, 2269 (1973).
(11) G. Harris, *Theor. Chim. Acta*, **10**, 119, 155 (1968).
(12) See, for example, G. Palmer and H. Brintzinger in "Electron and Coupled Energy Transfer in Biological Systems", T. E. King and M. Klingenberg, Ed., Vol. 1/Part B, Marcel Dekker, New York, N.Y., 1972, Chapter 9.
(13) C. D. Thorn and R. A. Ludwig, "The Dithiocarbamates and Related Compounds", Elsevier, Amsterdam, 1962.
(14) D. H. Turner, G. W. Flynn, N. Sutin, and J. V. Beitz, *J. Am. Chem. Soc.*, **94**, 1554 (1972).
(15) J. K. Beattie, N. Sutin, D. H. Turner, and G. W. Flynn, *J. Am. Chem. Soc.*, **95**, 2052 (1973).
(16) M. A. Hoselton, R. S. Drago, L. J. Wilson, and N. Sutin, *J. Am. Chem. Soc.*, **98**, 6967 (1976).
(17) M. F. Tweedle and L. J. Wilson, *J. Am. Chem. Soc.*, **98**, 4824 (1976).
(18) E. V. Dose, K. M. M. Murphy, and L. J. Wilson, *Inorg. Chem.*, **15**, 2622 (1976).
(19) M. G. Simmons and L. J. Wilson, *Inorg. Chem.*, **16**, 126 (1977).
(20) Since submission of this work for publication, a synthesis and characterization of the R = methyl derivative have appeared: H. Nakajima, T. Tanaka, H. Kobayashi, and I. Tsujikawa, *Inorg. Nucl. Chem. Lett.*, **12**, 689 (1976).
(21) Reference 17.
(22) B. L. Chrisman and T. A. Tumolillo, *Comput. Phys. Commun.*, **2**, 322 (1971).
(23) B. J. McCormick and B. P. Stormer, *Inorg. Chem.*, **11**, 729 (1972).
(24) See, for example, ref 9.
(25) R. J. Butcher and E. Sinn, *J. Am. Chem. Soc.*, **98**, 2440 (1976).
(26) R. Rickards and C. E. Johnson, *J. Chem. Phys.*, **48**, 5231 (1968).
(27) N. N. Greenwood and T. C. Gibb, "Mössbauer Spectroscopy", Chapman and Hall, London, 1971, p 63.
(28) A. H. Ewald, R. L. Martin, E. Sinn, and A. H. White, *Inorg. Chem.*, **8**, 1837 (1969).
(29) Reference 10.
(30) M. Sharrock, E. Münck, P. G. Debrunner, V. Marshall, J. D. Lipscomb, and I. C. Gunsalus, *Biochemistry*, **12**, 258 (1973).
(31) M. Cox, J. Darken, B. W. Fitzsimmons, A. W. Smith, L. F. Larkworthy, and K. A. Rogers, *J. Chem. Soc., Dalton Trans.*, 1192 (1972).
(32) M. J. Tricker, *J. Nucl. Chem.*, **36**, 1543 (1974).
(33) M. Das and S. E. Livingstone, *Aust. J. Chem.*, **27**, 2109 (1974).
(34) R. Beckett, G. A. Heath, B. F. Hoskins, B. P. Kelley, R. L. Martin, I. A. G. Roos, and P. L. Weickhardt, *Inorg. Nucl. Chem. Lett.*, **6**, 257 (1970).
(35) See, for example, ref 4, 15, 17, and 19.
(36) L. J. Wilson, D. Georges, and M. A. Hoselton, *Inorg. Chem.*, **14**, 2968 (1975); M. A. Hoselton, L. J. Wilson, and R. S. Drago, *J. Am. Chem. Soc.*, **97**, 1722 (1975).

Contribution from the Materials and Molecular Research Division, Lawrence Berkeley Laboratory, and the Department of Chemistry, University of California, Berkeley, California 94720

Synthesis, Crystal Structure, and Optical and Magnetic Properties of Tris[bis(N,N'-dimethylethylenediamido)uranium(IV)], a Trimeric Complex[1]

JOHN G. REYNOLDS, ALLAN ZALKIN,* DAVID H. TEMPLETON,* and NORMAN M. EDELSTEIN*

The trimeric compound U$_3$(CH$_3$NCH$_2$CH$_2$NCH$_3$)$_6$ was synthesized by the reaction of tetrakis(diethylamido)uranium(IV) with dimethylethylenediamine in pentane in a dry argon atmosphere. The crystals are monoclinic, space group $P2/a$, with $a = 17.019$ Å, $b = 9.932$ Å, $c = 11.013$ Å, $\beta = 107.45°$, and $d_{calcd} = 2.302$ g/cm^3 for $Z = 2$. X-ray diffraction intensity data were collected by an automated diffractometer using graphite-monochromated Mo Kα radiation. For 1044 reflections with $F^2 > 3\sigma(F^2)$, $R_1 = 0.047$ and $R_2 = 0.036$. The three uranium atoms form a linear chain with the central one, which is on a center of symmetry, being linked by a triple-nitrogen bridge to each of the terminal ones. The uranium–uranium distance is 3.543 Å. Each of the bridge nitrogen atoms comes from a different dimethylethylenediamine and gives the central uranium atom an octahedron of six nitrogen nearest neighbors at an average distance of 2.37 Å. The terminal uranium atom is at the center of a distorted trigonal prism of its neighbors; there are three bridge bonds and three single bonds with average distances of 2.57 and 2.21 Å, respectively. Optical and near-IR spectra of various solutions are reported; these data suggest the molecule is also trimeric in solution. The magnetic susceptibility of U$_3$(CH$_3$NCH$_2$CH$_2$NCH$_3$)$_6$ follows the Curie–Weiss law in the temperature range 4.6–100 K with no evidence of magnetic ordering. This trimeric structure is novel in actinide structural chemistry.

Introduction

We recently reported the crystal structure and magnetic and optical properties of uranium diethylamide,[2a] the first well-characterized actinide dialkylamide.[2b] This molecule in the solid state is dimeric and has an unusual five-coordination about the U atoms. Other uranium amides had been syn-

thesized but none had been isolated as pure compounds. The usual method of purification for d transition metal amides is by distillation or sublimation but this method has been unsuccessful for other uranium amides. We have speculated this is due to a greater degree of oligomerization for dialkylamides in the actinide series than in the d transition series. Generally,
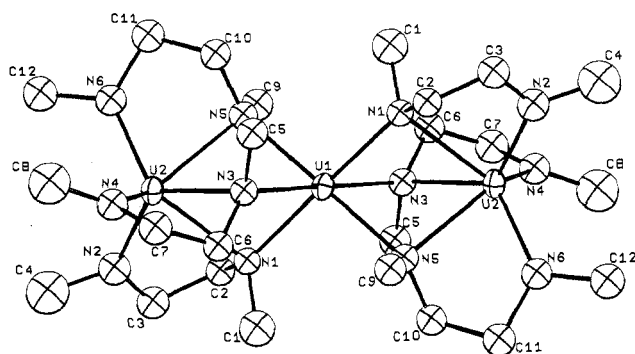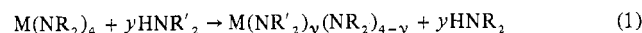
Figure 1. Molecular structure of $U_3(dmed)_6$.

the synthesis of transition metal alkylamides is by the reaction of the transition metal halide with the corresponding lithium dialkylamide. This method was used by Jones et al.[2b] to prepare $U(NEt_2)_4$. However, Bradley and co-workers have also used an aminolysis reaction

$$M(NR_2)_4 + yHNR'_2 \rightarrow M(NR'_2)_y(NR_2)_{4-y} + yHNR_2 \tag{1}$$

in some instances.[3] We report in this paper the synthesis of uranium dimethylethylenediamine by this method, its crystal structure, and optical and magnetic properties.

Experimental Section

Reagents and Syntheses. All solvents were dried by refluxing with Na and benzophenone in an argon atmosphere. Materials were handled in an argon atmosphere glovebox or on a vacuum line.

$U(NEt_2)_4$. This compound was prepared as described previously.[2a]

Dimethylethylenediamine (Bp 119 °C, Density 0.828). This compound was purchased from the Aldrich Chemical Co., dried over CaH_2, and then distilled and degassed before use.

Reaction of $U(NEt_2)_4$ with N,N'-Dimethylethylenediamine. A 3.5-g sample of $U(NEt_2)_4$ was placed in a 250-ml Schlenk flask. Approximately 100 ml of dry pentane was vacuum-distilled into the flask at 77 K. After the addition of the pentane was complete, the dimethylethylenediamine was added under vacuum. The reaction mixture was allowed to warm to room temperature while being stirred. After approximately 24 h the precipitate was filtered and vacuum-dried. Crystals were grown from the filtrate. The major fraction of the crystals obtained were monoclinic and yellow and are shown below to be the trimer $U_3(CH_3NCH_2CH_2NCH_3)_6$ or $U_3(dmed)_6$. However, it was possible to isolate a minor fraction which were orthorhombic and red-brown. Recrystallization of the precipitate from pentane yielded additional yellow crystals which were identical with the yellow crystals from the filtrate. No red-brown crystals were obtained from solutions prepared from the precipitate. $U_3(dmed)_6$ was not volatile below 120 °C and decomposed above this temperature.

Physical Measurements. For optical measurements a weighed amount of $U_3(dmed)_6$ was dissolved in benzene to form a $\sim$0.02 M solution. A saturated solution of $U_3(dmed)_6$ in diethyl ether was prepared. The solutions were put in 0.5-cm cells in an inert-atmosphere box and sealed with wax. All measurements were obtained on a Cary 17 spectrophotometer containing only the solvent in a 0.5-cm cell in the reference compartment.

Magnetic susceptibility measurements were obtained with a PAR Model 155 vibrating-sample magnetometer used with a homogeneous magnetic field produced by a Varian Associates 12-in. electromagnet capable of a maximum field strength of 12.5 kG. The magnetometer was calibrated with $HgCo(CNS)_4$.[4] A variable-temperature liq-

uid-helium Dewar produced sample temperatures in the range 4.2–100 K which were measured by a calibrated GaAs diode placed approximately 0.5 in. above the sample.

X-Ray Diffraction. A tungsten needle was used to insert a few crystals into quartz capillaries in an inert-atmosphere box and the capillaries were then fire sealed under vacuum. A sealed capillary was mounted on a Picker FACS-I automated diffractometer equipped with a graphite monochromator and molybdenum tube. The cell dimensions were obtained by a least-squares refinement procedure from the angular positions of 12 manually centered reflections for which $K\alpha_1$ peaks were resolved. The space group and cell dimensions are given in Table I with some other details of the experiment. ω scans of several low-angle reflections showed widths of half-peak height of about $^1/_8°$. A total of 4983 scans were measured and later averaged to give a set of 2342 unique reflections. Three standard reflections were measured after each 200th scan to monitor for crystal decay, instrumental stability, and crystal alignment. After 8 days of data-taking the standards exhibited no measurable decay in intensity and fluctuated by about 1% from their average values.

Absorption corrections were calculated using an analytical algorithm.[5] The measurement of the physical dimensions of the crystal was somewhat hampered by its containment inside a capillary. The crystal shape was described by six surface planes. Azimuthal scans of integrated intensity were performed for seven different reflections in as diverse a region of reciprocal space as the instrument would allow, and the dimensions of the crystal were adjusted to give the best consistency of corrected intensities for these scans. The data were processed, averaged, and given estimated standard deviations using formulas presented in the supplementary material. The factor $p = 0.02$ was used in the calculation of $\sigma(F^2)$.

The Patterson function revealed the uranium atom positions, and the subsequent electron density Fourier map, phased by the uranium atoms, gave the positions of all of the nitrogen and carbon atoms. The structure was refined by full-matrix least squares where the function $\sum w\|F_o\| - |F_c\|^2$ was minimized. About 20 reflections below $(\sin\theta)/\lambda$ of 0.125 were given zero weight because a few of them had excessively large discrepancies; these discrepancies were mainly in the region where the background peaked due to scattering from the quartz capillary. No correction for extinction was indicated, and none was made.

In the final least-squares refinements, only the two U atoms were given anisotropic thermal parameters. Earlier attempts to treat the carbon and nitrogen atoms anisotropically did not result in any significant improvements of the R factors, and some of the thermal tensors did not remain positive-definite. The intensities are relatively weak due to the very small crystal size, and the anisotropic description of the light atoms is not feasible with this data set. A difference Fourier map calculated after the last least-squares cycle showed peaks of 2.8 $e/Å^3$ or less. The final R factor, $\sum \|F_o\| - |F_c\|/\sum|F_o|$, was 0.047 for 1044 data where $F^2 > 3\sigma(F^2)$ and 0.135 for all 2342 data. The weighted R_w factor, $(\sum w(\Delta F)^2/\sum wF_o^2)^{1/2}$, was 0.036. The standard deviation of an observation of unit weight was 1.09.

Final positional and thermal parameters are given in Table II; a table of observed structure factor amplitudes is given in the supplementary material; and distances and angles are listed in Tables III and IV.

Discussion

The structure analysis shows that the U(IV) complex with dimethylethylenediamine is a cluster containing three uranium atoms in a line bridged by nitrogen atoms; see Figures 1 and 2. The central uranium atom is on a center of symmetry and is 3.543 Å from the terminal atoms. The uranium atoms are joined by triple nitrogen bridge bonds, each of which is from
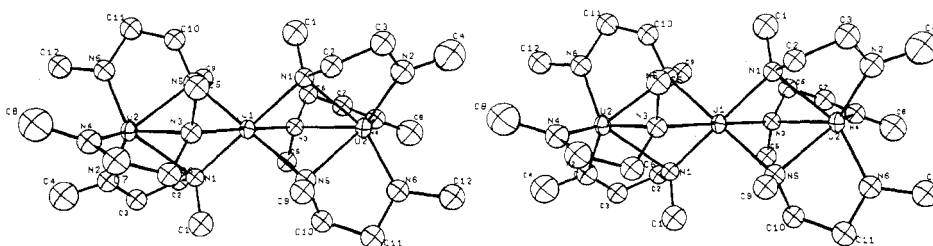

Figure 2. Stereoview of the complex.

Tris[bis(*N,N'*-dimethylethylenediamido)uranium(IV)]

Table I. Summary of Crystal Data and Intensity Collection

Compd	$U_3(CH_3NCH_2CH_2NCH_3)_6$
Fw	1230.9
a	17.019 (7) Å
b	9.932 (4) Å
c	11.013 (5) Å
β	107.45 (5)°
V	1776 Å³
Z	2
Density (calcd)	2.302 g/cm³
Space group[a]	$P2/a$ (alternate setting of $P2/c$)
Crystal shape and size	Approximate parallelepiped of 6 faces: 020, 0$\bar{2}$0, 002, 200, $\bar{2}$01, 00$\bar{2}$; dimensions 0.04 × 0.05 × 0.09 mm
Crystal vol	0.000 182 mm³
Temp	23 °C
Radiation	Mo Kα (λ 0.709 26 and 0.713 54 Å), monochromated from (002) face of mosaic graphite
Transmission factor	0.32–0.60
μ	131 cm⁻¹
Data collection method	θ–2θ scan (1°/min along 2θ)
Scan range	0.7° below Kα₁ to 0.7° above Kα₂
Background counts	8-s backgrounds offset from scan limits by 0.5°
2θ limits	3–45°
Final no. of variables	91
Unique data used ($F_o^2 > 3\sigma(F_o^2)$; $(\sin\theta)/\lambda > 0.125$)	1044

[a] The general positions are ±(x, y, z; ½ + $x, -y, z$).

Table II. Positional and Thermal Parameters[a]

	x	*y*	*z*	*B*, Å²
U(1)	0	0	0	
U(2)	0.047 05 (6)	0.2295 (1)	0.2582 (1)	
N(1)	0.073 (1)	0.206 (2)	0.039 (2)	2.5 (4)
N(2)	0.137 (1)	0.387 (3)	0.239 (2)	3.7 (5)
N(3)	−0.081 (1)	0.134 (2)	0.095 (2)	2.6 (5)
N(4)	−0.064 (1)	0.332 (2)	0.278 (2)	3.4 (5)
N(5)	0.073 (1)	−0.019 (2)	0.220 (2)	2.9 (4)
N(6)	0.104 (1)	0.131 (2)	0.441 (2)	3.3 (5)
C(1)	0.035 (2)	0.308 (3)	−0.065 (3)	4.5 (7)
C(2)	0.164 (1)	0.239 (3)	0.085 (2)	2.9 (5)
C(3)	0.183 (2)	0.376 (3)	0.151 (3)	3.7 (6)
C(4)	0.155 (2)	0.511 (4)	0.313 (3)	6.5 (8)
C(5)	−0.134 (2)	0.042 (3)	0.143 (3)	3.5 (6)
C(6)	−0.123 (1)	0.266 (3)	0.060 (2)	3.2 (5)
C(7)	−0.146 (2)	0.328 (3)	0.170 (3)	3.9 (7)
C(8)	−0.078 (2)	0.387 (4)	0.394 (3)	6.2 (9)
C(9)	0.156 (2)	−0.073 (3)	0.230 (3)	3.6 (6)
C(10)	0.050 (1)	−0.074 (3)	0.330 (3)	3.2 (6)
C(11)	0.107 (1)	−0.024 (3)	0.465 (2)	3.7 (7)
C(12)	0.152 (1)	0.207 (3)	0.564 (3)	4.2 (6)

	B_{11}	B_{22}	B_{33}	B_{12}	B_{13}	B_{23}
U(1)	1.81 (7)	2.5 (1)	2.04 (8)	−0.05 (7)	0.66 (5)	−0.34 (9)
U(2)	2.11 (4)	2.54 (7)	2.17 (5)	0.06 (5)	0.36 (3)	−0.46 (6)

[a] The anisotropic temperature factor has the form $\exp[-0.25(B_{11}h^2a^{*2} + 2B_{12}hka^*b^* + \ldots)]$.

Table III. Interatomic Distances[a] (Å)

U(1)–U(2)	3.543 (1)	N(2)–C(3)	1.43 (3)
–N(1)	2.37 (2)	–C(4)	1.46 (4)
–N(3)	2.37 (2)	N(3)–C(5)	1.48 (3)
–N(5)	2.38 (2)	–C(6)	1.49 (3)
U(2)–N(2)	2.24 (2)	N(4)–C(7)	1.54 (3)
–N(4)	2.21 (2)	–C(8)	1.47 (4)
–N(6)	2.19 (2)	N(5)–C(9)	1.48 (3)
–N(1)	2.60 (2)	–C(10)	1.49 (3)
–N(3)	2.55 (2)	N(6)–C(11)	1.57 (4)
–N(5)	2.57 (2)	–C(12)	1.54 (3)
N(1)–C(1)	1.52 (3)	C(2)–C(3)	1.53 (4)
–C(2)	1.51 (3)	C(6)–C(7)	1.51 (3)
		C(10)–C(11)	1.58 (4)

[a] Uncorrected for thermal motion.

Table IV. Selected Angles (deg)

U(2)–U(1)–U(2)'	180.0	U(1)–N(1)–C(2)	133 (2)
N(1)–U(1)–N(3)	77.2 (7)	U(1)–N(3)–C(5)	108 (2)
N(1)–U(1)–N(5)	78.4 (8)	U(1)–N(3)–C(6)	133 (2)
N(3)–U(1)–N(5)	78.0 (7)	U(1)–N(5)–C(9)	107 (2)
N(1)–U(1)–N(3)'	102.8 (7)	U(1)–N(5)–C(10)	133 (2)
N(1)–U(1)–N(5)'	101.6 (8)	U(2)–N(1)–C(1)	119 (2)
N(3)–U(1)–N(5)'	102.0 (7)	U(2)–N(1)–C(2)	96 (1)
N(1)–U(1)–N(1)'	180.0	U(2)–N(3)–C(5)	117 (2)
N(3)–U(1)–N(3)'	180.0	U(2)–N(3)–C(6)	96 (2)
N(5)–U(1)–N(5)'	180.0	U(2)–N(5)–C(9)	123 (2)
N(1)–U(2)–N(3)	70.1 (6)	U(2)–N(5)–C(10)	97 (2)
N(1)–U(2)–N(5)	71.1 (7)	C(1)–N(1)–C(2)	106 (2)
N(3)–U(2)–N(5)	71.3 (6)	C(5)–N(3)–C(6)	109 (2)
N(1)–U(2)–N(2)	70.2 (7)	C(9)–N(5)–C(10)	106 (2)
N(3)–U(2)–N(4)	70.6 (7)	U(2)–N(2)–C(3)	123 (2)
N(5)–U(2)–N(6)	70.8 (7)	U(2)–N(2)–C(4)	125 (2)
N(1)–U(2)–N(4)	121.5 (7)	C(3)–N(2)–C(4)	112 (2)
N(1)–U(2)–N(6)	131.7 (7)	U(2)–N(4)–C(7)	121 (2)
N(3)–U(2)–N(6)	130.8 (7)	U(2)–N(4)–C(8)	128 (2)
N(3)–U(2)–N(6)	122.3 (8)	C(7)–N(4)–C(8)	110 (2)
N(5)–U(2)–N(2)	120.0 (7)	U(2)–N(6)–C(11)	125 (2)
N(5)–U(2)–N(4)	130.8 (7)	U(2)–N(6)–C(12)	124 (2)
N(2)–U(2)–N(4)	108.3 (9)	C(11)–N(6)–C(12)	111 (2)
N(2)–U(2)–N(6)	105.6 (8)	N(1)–C(2)–C(3)	114 (2)
N(4)–U(2)–N(6)	105.9 (8)	N(3)–C(6)–C(7)	112 (2)
U(1)–N(1)–U(2)	90.9 (6)	N(5)–C(10)–C(11)	115 (2)
U(1)–N(3)–U(2)	92.1 (6)	N(2)–C(3)–C(2)	108 (2)
U(1)–N(5)–U(2)	91.5 (7)	N(4)–C(7)–C(6)	104 (2)
U(1)–N(1)–C(1)	111 (2)	N(6)–C(11)–C(10)	100 (2)

a different dimethylethylenediamine ligand. This trimer type structure is novel in actinide structural chemistry, and even dimeric complexes are relatively rare for uranium.

The two uranium atoms in this compound have considerably different environments. The central uranium atom is on a center of symmetry with six chemically equivalent nitrogen atoms about it at the corners of an elongated trigonal antiprism. The average U(1)–N distance is 2.37 Å. The terminal uranium atom, U(2), is at the center of the distorted trigonal prism of six nitrogen atoms, including both nitrogen atoms of each of three dimethylethylenediamine ligands. The six nitrogen neighbors of the terminal uranium atom define a figure which is closer to a trigonal prism than to a regular octahedron. Atoms N(1), N(3), and N(5) are nearly at the corners of an equilateral triangle of edge 2.98 Å, while N(2), N(4), and N(6) nearly define a similar triangle of edge 3.55 Å. These two triangles are rotated about 8° from eclipsed orientations. For each ligand one nitrogen is bridging and the other is terminal. The average bridge- and terminal-bond distances are 2.57 and 2.21 Å, respectively. As is expected, the U–N distances are greater for bridging nitrogen atoms than for terminal nitrogen atoms. The bridge-bond lengths found in this compound and in the dimer of uranium(IV) diethylamide[2a] have a considerable range of values. This variation may be understood if one considers the bond orders assigned on the basis of electrostatic bonding. Assuming that each uranium is involved in a total of four bonds, then each U(1)–N is a two-thirds bond, the U(2)–N bridges are each one-third bond, and the U(2)–N terminal bonds are each one bond. With this assignment the average single bond is 2.21 Å, a two-thirds bond is 2.37 Å, and a one-third bond is 2.57 Å. In $U_2(Et_2N)_8$[2] the bridge is a half-bond and has an average distance of 2.51 Å, while the terminal single bonds average 2.22 Å.

While the bonds for the bridging nitrogen atom are approximately tetrahedral, those of the terminal ones are very nearly coplanar. Each terminal nitrogen atom is within 0.1 Å of the plane defined by uranium and the two α-carbon atoms. Although at first glance there appears to be a large range of values for the N–C bond lengths, the variation from maximum to minimum values are 3–4 esd's and are not experimentally significant.
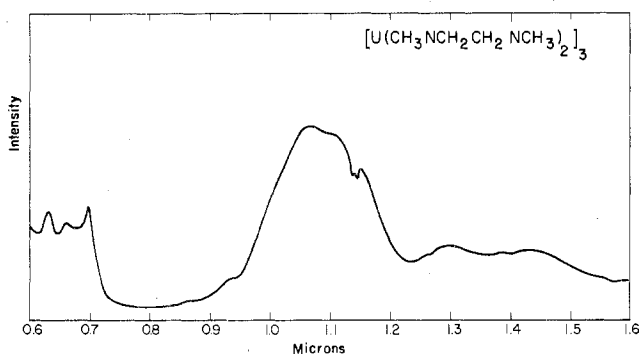
Figure 3. Optical spectrum of $U_3(dmed)_6$ in C_6H_6.

Table V. Optical Spectra of $U_3(dmed)_6$

$U_3(dmed)_6$ in C_6H_6		$U_3(dmed)_6$ in Et_2O	
$\lambda, \mu m$	ϵ	$\lambda, \mu m$	ϵ^a
0.631	74	0.630	52
0.661	67	0.661	49
0.699	79	0.699	65
0.935	29	0.931	25
1.065	134	1.060	134
1.111	127	1.105	127
1.145	99		
1.153	104	1.150	104
1.300	50	1.300	53
1.431	47	1.438	51

^{a} Calculated assuming the intensity of the peak at 1.06 μm is the same in C_6H_6 and Et_2O.

The rod-shaped molecules pack in this crystal in a manner similar to that found in the tetragonal structure of dimethylacetylene[6] and krypton difluoride.[7] Molecules with centers at $x = 0$ lie in a nearly square array with their axes all oriented approximately along one of the diagonals of the square. The next layer (at $x = {}^1/_2$) is similar, but the molecular axes are nearly perpendicular to those in the first layer. The molecular centers are arranged according to the pattern of cubic closest packing, but with considerable distortion from ideal cubic geometry.

The aminolysis reaction (1) can be considered an acid–base reaction where the HNR'_2 is considered to be the acid, and the amide on the metal is the base. If the two amide groups make equally strong bonds to uranium, the driving force for the reaction would then depend on the difference between the pK_a's of the amines. Unfortunately, there are no quantitative measurements for the pK_a's of the amines discussed in this paper and involved in reaction 1, but qualitatively, it appears the second nitrogen in the dimethylethylenediamine acts as an electron-withdrawing group which lowers the first pK_a of dimethylethylenediamine with respect to diethylamine. The second significant factor in this reaction is the chelate effect which results in the enhanced stability of the complex which contains chelate rings when compared to a similar system without rings.[8] The driving force for the formation of this U trimer is probably due to some combination of the above effects.

The optical and near-IR spectrum of $U_3(dmed)_6$ in benzene is shown in Figure 3. The extinction coefficients of the peaks are listed in Table V. Although we did not obtain quantitative optical data on $U_3(dmed)_6$ in diethyl ether, we can calculate approximate values for the extinction coefficients by assuming the extinction coefficient for the strongest peak is the same as in benzene and then calculate the other extinction coefficients relative to the strongest peak. These values are also listed in Table V. The general features of the spectra in benzene or in diethyl ether are identical unlike the spectra of $U(NEt_2)_4$ in these two solvents. In the latter case we attributed
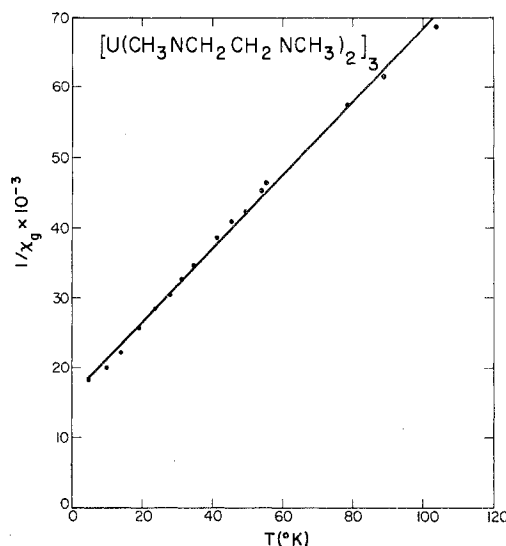

Figure 4. Inverse gram-susceptibility of $U_3(dmed)_6$ vs. temperature. The straight line is the calculated inverse gram-susceptibility in that temperature range with the parameters obtained from a least-squares fit as given in the text.

the differences between the optical and ^1H NMR spectra in the two solvents to the complexing of monomeric $U(NEt_2)_4$ by the coordinating ether solvent. The close similarity of the spectra of $U_3(dmed)_6$ in the two solvents suggests that the molecule is trimeric in solution with the coordination sites on the U atoms filled or effectively blocked by the ligands.

The inverse of the gram magnetic susceptibility of U_3-$(dmed)_6$ in the temperature range 4.6–100 K is shown in Figure 4. The susceptibility follows the Curie–Weiss law

$$\chi_M = C_M/(T + \Theta)$$

with $C_M = 0.78$, μ_{eff}(per U atom) $= 2.50 \mu_B$, and $\Theta = 30.5$ K, throughout the measured temperature range. The magnetic data can be explained empirically by a doublet crystalline field level as the ground state with the splitting of this doublet (if any) less than ~ 5 cm^{-1}. Let us consider only the symmetry about each of the U ions as determined by the neighboring U ions and the N atoms. The axis determined by the line joining the three U atoms is a threefold axis with the center U atoms at a site of D_{3d} symmetry and the terminal U atoms (equivalent by symmetry) at sites of approximately C_{3v} symmetry. For the $^3H_4$ (LS coupling) ground term of U^{4+}, each of the above symmetries will split a $J = 4$ term into three doublets and three singlets.[9] We consider the empirical magnetic susceptibility as the sum of the susceptibilities of each of the ions. The measured results are consistent with a doublet state being lowest for each of the two inequivalent sites. There is no indication of magnetic ordering in this trimeric molecule in the measured temperature range.

The most striking feature of $U_3(dmed)_6$ is the linear array of three U atoms bridged by six dimethylethylenediamine groups. Only one amide nitrogen atom of each dimethylethylenediamine is bridging, the other terminal nitrogen atom forming a planar bond between a uranium atom and a carbon atom. Further evidence for the tendency to bridge in the uranium amides is given by the preliminary x-ray diffraction results for the minor red-brown product. This compound forms a puckered rectangle of four U atoms with U–U distances of approximately 3.6 Å. The U atoms in this structure are also bridged by the dimethylethylenediamine groups. The evidence to date suggests that for the uranium amides, if the R groups of the amide are not bulky enough to prevent bridging through steric hindrance as, for example, found in $U(NPh_2)_4$,[10] oligomers of the uranium amides will be formed. We have

suggested previously[2a] that bridging through the amide nitrogen more readily takes place in the actinide series than in the early d transition series because of a reduced ligand $p\pi$ to metal orbital π interaction in the f series. This reduction allows the amide nitrogen atom to more easily become tetrahedral and act as a bridging atom. Consequently the actinide amides may tend to oligomerize and/or be more thermally unstable than analogous d transition compounds. The recent report of the isolation of $Zr(N(i\text{-}Pr)_2)_4$ by sublimation at 120 °C (10^{-3} mmHg)[11] supports this suggestion since the analogous U compound was not isolated by Jones et al.[2b] nor by our group to date. However, much work remains to be done on these compounds in both f and d transition series.

Registry No. $U_3(dmed)_6$, 61202-81-1; $U(NEt_2)_4$, 40678-59-9.

Supplementary Material Available: Listings of structure factors and formulas used in data reduction (10 pages). Ordering information is given on any current masthead page.

References and Notes
(1) This work was done with support from the U.S. Energy Research and Development Administration.
(2) (a) J. G. Reynolds, A. Zalkin, D. H. Templeton, N. M. Edelstein, and L. K. Templeton, *Inorg. Chem.*, **15**, 2498 (1976); (b) R. G. Jones, G. Karmas, G. A. Martin, Jr., and H. Gilman, *J. Am. Chem. Soc.*, **78**, 4285 (1956).
(3) For a review of metal dialkylamides and the methods of synthesis see D. C. Bradley, *Adv. Inorg. Chem. Radiochem.*, **15**, 259 (1972).
(4) H. St. Rade, *J. Phys. Chem.*, **77**, 424 (1973).
(5) L. K. Templeton and D. H. Templeton, Abstracts, American Crystallographic Association Proceedings, Series 2, Vol. 1, 1973, p 143.
(6) E. Pignataro and B. Post, *Acta Crystallogr.*, **8**, 672 (1955).
(7) R. D. Burbank, W. E. Falconer, and W. A. Sunder, *Science*, **178**, 1285 (1972).
(8) F. A. Cotton and G. Wilkinson, "Advanced Inorganic Chemistry", 3d ed, Interscience, New York, N.Y., 1972, p 650.
(9) G. F. Koster, J. O. Dimmock, R. G. Wheeler, and H. Statz, "Properties of the Thirty-Two Point Groups", M.I.T. Press, Cambridge, Mass., 1963.
(10) J. G. Reynolds, A. Zalkin, D. H. Templeton, and N. M. Edelstein, to be submitted for publication.
(11) C. Airoldi and D. C. Bradley, *Inorg. Nucl. Chem. Lett.*, **11**, 155 (1975).

The Tungsten–Tungsten Triple Bond. 6. Hexakis(*N,N*-dimethylcarbamato)ditungsten and Dimethyltetrakis(*N,N*-diethylcarbamato)ditungsten. Structures and Dynamical Solution Behavior

MALCOLM H. CHISHOLM,*[1a] F. ALBERT COTTON,*[1b] MICHAEL W. EXTINE,[1a] and B. RAY STULTS[1b]

$W_2(NMe_2)_6$ and $W_2Me_2(NEt_2)_4$ each react with carbon dioxide to give $W_2(O_2CNMe_2)_6$, I, and $W_2Me_2(O_2CNEt_2)_4$, II, respectively. Single-crystal x-ray structural analyses show that both I and II are dinuclear and contain tungsten to tungsten triple bonds (W≡W_{av} = 2.275 Å) bridged by two dialkylcarbamato, O_2CNR_2, ligands. Crystal parameters are as follows: $W_2(O_2CNMe_2)_6$, $P\bar{1}$, a = 12.018 (2) Å, b = 16.516 (4) Å, c = 11.630 (3) Å, α = 111.09 (2)°, β = 107.26 (2)°, γ = 91.00 (2)°, Z = 2; R_1 = 0.073; for $W_2Me_2(O_2CNEt_2)_4$, $P2_1/c$, a = 16.014 (4) Å, b = 10.433 (4) Å, c = 18.983 (5) Å, β = 107.51 (2)°, Z = 4, R_1 = 0.040. In both compounds each tungsten atom is at the apex of an irregular pentagonal pyramid. The basal vertices of each pyramid are defined by the two oxygen atoms of the bidentate nonbridging carbamato ligand (W–O_{av} = 2.16 Å), one oxygen atom from each of the two bridging carbamato groups (W–O_{av} = 2.08 Å), and either an oxygen atom from the other carbamato ligand (W–O_{av} = 2.07 Å) in compound I or a methyl group (W–C_{av} = 2.20 Å) in compound II. In compound I, the second oxygen atom from the nonbridging carbamato ligand is weakly bonded (W–O_{av} = 2.67 Å) along an extension of the tungsten-to-tungsten triple bond. NMR studies show that, while I and II retain their structures in solution, both molecules are fluxional. The low-temperature ^{1}H NMR spectra for $W_2(O_2CNMe_2)_6$ provide a slow-exchange limiting spectrum at –60 °C, consisting of four signals of relative intensities 4:4:2:2, consistent with the structure found in the solid state which has approximate C_{2v} symmetry. As the temperature is raised, these four signals are seen to collapse and eventually re-form as a sharp singlet (+70 °C) showing that all three ligands undergo rapid scrambling. The low-temperature limiting ^{13}C NMR spectrum (–60 °C) consists of three resonances of relative intensities 1:1:1 assignable to the carboxylic carbons and four resonances of relative intensities 4:4:2:2 assignable to the methyl carbons. As the temperature is raised, three processes are observed, which are, in order of increasing energy, (i) the interchange of proximal and distal methyl groups of the unsymmetrically bonded bidentate O_2CNMe_2 ligand, (ii) interchange of the nonbridging ligands, and (iii) interchange of nonbridging and bridging carbamato ligands. Variable-temperature ^{1}H NMR studies on $W_2Me_2(O_2CNEt_2)_4$ indicate that at +80 °C exchange between bridging and nonbridging carbamato ligands is rapid on the NMR time scale.

Introduction

Tungsten, unlike its neighbors molybdenum and rhenium, has not yet been shown conclusively to form compounds containing metal-to-metal quadruple bonds,[2] despite the existence of scores of well-characterized, quadruply bonded compounds for molybdenum and rhenium.[2a] However, recent work from our laboratories has shown that there exists an extensive series of compounds containing tungsten-to-tungsten triple bonds, e.g., $W_2(NR_2)_6$, where R = Me[3] and Et,[3] and $W_2(NEt_2)_4X_2$, where X = Cl,[4] Br,[5] I,[5] Me,[6] and CH_2SiMe_3.[5] There is also the compound $W_2(CH_2SiMe_3)_6$ reported first by Wilkinson[7] and recently structurally characterized by us.[8] In addition, the alkoxides $W_2(OR)_6$,[9] where R = *t*-Bu and SiMe₃, appear to be members of a structurally related series M_2L_6,

where M = Mo and W and L = R (alkyl),[10] NR_2,[11] and OR,[12] containing metal-to-metal triple bonds unsupported by bridging ligands. In the preceding paper[5] we described chlorine atom substitution reactions involving $W_2Cl_2(NEt_2)_4$: an extensive chemistry of compounds of the type $W_2X_2(NEt_2)_4$ where X is a univalent anionic ligand was implicated. The transition metal–nitrogen bond in early transition metal dialkylamides, $M(NR_2)_n$, is known to be reactive toward a number of exchange and insertion reactions.[13] Thus an extension of the dinuclear chemistry of trivalent tungsten might be anticipated from the compounds $W_2(NR_2)_6$ and $W_2X_2(NR_2)_4$. In this paper we describe our characterization of $W_2(O_2CNMe_2)_6$, I, and $W_2Me_2(O_2CNEt_2)_4$, II, formed by the reactions of carbon dioxide with $W_2(NMe_2)_6$ and $W_2Me_2(NEt_2)_4$, re-